Dynamic and Control in a Three-Variable Chemical Reaction Model

Marcio Demetrius Martinez[1,2,#] and Fábio Roberto Chavarette[2,*,#]

[1] State University of Mato Grosso do Sul (UEMS), Naviraí, Mato Grosso do Sul, 79950-000, Brazil

[2] School of Engineering, São Paulo State University (UNESP), Ilha Solteira, São Paulo, 15385-007, Brazil

[#] These authors contributed equally to this work

INFORMATION

Keywords:
Chemical reactions
dynamical model
chaos
control

DOI: 10.23967/j.rimni.2025.10.67551

SCIPEDIA Revista Internacional de Métodos Numéricos para Cálculo y Diseño en Ingeniería

Revista Internacional Métodos numéricos para cálculo y diseño en ingeniería RIMNI

In cooperation with CIMNE

Dynamic and Control in a Three-Variable Chemical Reaction Model

Marcio Demetrius Martinez[1,2,#] **and Fábio Roberto Chavarette**[2,*,#]

[1]State University of Mato Grosso do Sul (UEMS), Naviraí, Mato Grosso do Sul, 79950-000, Brazil

[2]School of Engineering, São Paulo State University (UNESP), Ilha Solteira, São Paulo, 15385-007, Brazil
[#]These authors contributed equally to this work

ABSTRACT

Chaotic behavior in nonlinear chemical systems presents significant challenges for stability and control, particularly in practical applications. This study investigates the suppression of chaos in a three-variable reaction system through an optimal linear feedback strategy, formulated via the solution of an algebraic Riccati equation. The proposed control approach effectively eliminates chaotic oscillations, guiding the system to equilibrium even under parameter uncertainties of up to 20%. Numerical simulations confirm that the control action maintains high robustness, ensuring convergence with minimal effort. The stabilization time for x_1 remains close to 29 s across different tolerances, while x_2 and x_3 converge nearly instantly, demonstrating the rapid effectiveness of the method. Furthermore, the control signal stabilizes at a small positive value after a short transient, reinforcing the computational efficiency and practical feasibility of this approach. These findings demonstrate that optimal linear control techniques provide a reliable and theoretically sound framework for managing nonlinear chemical systems, offering an accessible solution for real-world applications in engineering and process optimization.

OPEN ACCESS

Received: 06/05/2025

Accepted: 10/07/2025

Published: 27/10/2025

DOI
10.23967/j.rimni.2025.10.67551

Keywords:
Chemical reactions
dynamical model
chaos
control

1 Introduction

Chemical reaction models represent an essential class of systems in nonlinear dynamics, often used to analyze time-dependent behavior in chemical and biochemical processes. The stagnation point is a critical factor in reaction rates and material deposition, hence research on this topic is essential for optimising processes like chemical reactors and coating applications [1]. These models can display rich and diverse phenomena such as oscillations, multistability, and chaos, which are fundamental to understanding the behavior of many physical and biological systems. A prominent case is the Belousov–Zhabotinsky (BZ) reaction, frequently adopted as a reference for investigating self-organized oscillations and spatiotemporal complexity in reactive media [2]. Inspired by such models, researchers have explored more sophisticated systems, including the three-variable chemicalreaction model introduced by Li and Xu [3]. More recently, Martinez and Chavarette analyzed a four-dimensional system composed of Michaelis–Menten-type nonlinearities, demonstrating the emergence

*Correspondence: Fábio Roberto Chavarette (fabio.chavarette@unesp.br)

of hyperchaos and proposing a control method based on optimal linear design, capable of maintaining performance even under parameter uncertainties [4,5].

The relevance of chaotic dynamics in chemical kinetics has increased in recent years, as numerous reactive systems have been shown to exhibit sensitive dependence on initial conditions and irregular long-term behavior. These properties, although deterministic in nature, result from the nonlinear structure of the governing equations. Since some dynamic features are not directly observable through experimental measurements, mathematical modeling and numerical analysis have become essential tools in the characterization of such systems [6], especially when considering additional complexities such as heat flux, variable thermal conductivity, and chemical reactions under external forces [7].

From a practical standpoint, the suppression or control of chaotic behavior in chemical reactors is an important problem in process engineering. Diverse control methodologies—ranging from classical Proportional-Integral-Derivative (PID) control to adaptive, predictive, feedback linearization, fuzzy logic, neural networks, and optimal control—have been developed and successfully applied to stabilize systems with oscillatory or chaotic dynamics [8]. The selection of a suitable control approach depends on the nature of the process, the operating constraints, and the performance objectives, such as improving productivity or reducing costs [9].

This study focuses on a three-dimensional chemical model that incorporates two Michaelis–Menten-type reactions [3,10]. The system is known to exhibit chaotic behavior under specific parameter settings. We propose the application of a state feedback control strategy derived from optimal control theory, based on the method developed by Rafikov and Balthazar [11], which relies on solving an algebraic Riccati equation to obtain a control law that minimizes a quadratic performance index.

To diagnose chaotic behavior, we compute the system's Lyapunov exponents using the algorithm proposed by Wolf et al. [12]. This technique estimates divergence rates between nearby trajectories in phase space, providing a quantitative indicator of chaos. As emphasized in nonlinear dynamics literature [13], the presence of one positive exponent, one zero, and one negative (a $[+, 0, -]$ spectrum) is a typical signature of chaotic attractors in three-dimensional dissipative systems.

Moreover, we analyze the frequency characteristics of the system's trajectories to complement the time-domain observations. Periodic signals are associated with discrete frequency components, whereas chaotic responses yield broadband spectra. Although spectral analysis alone cannot confirm the presence of chaos, it is useful for identifying transitions and bifurcations that may lead to qualitative changes in system behavior [14].

In summary, this study aims to contribute to the advancement of nonlinear dynamical system control, particularly in the context of chemical reactions described by Michaelis–Menten kinetics, by applying an optimal linear control strategy based on the Riccati equation. The originality of this approach lies in the integration of a classical linear control technique into a highly nonlinear system that is sensitive to parametric uncertainties and exhibits confirmed chaotic dynamics. While previous studies have often focused on chaos analysis or employed more complex techniques such as adaptive and fuzzy control, this research demonstrates that chaotic oscillations can be suppressed in a robust, efficient manner with minimal control effort, even under random parameter variations of up to 20%. Beyond validating the effectiveness of the proposed approach through numerical simulations and rigorous dynamical analysis tools, such as Lyapunov exponents and Poincaré maps, this work fills a research gap by offering a theoretically sound, computationally accessible, and potentially applicable solution for industrial processes, where parameter uncertainties are an inherent practical challenge. The results reinforce that the proposed method not only stabilizes chaotic dynamics but also expands the possibilities for controlling dissipative chemical systems in real-world scenarios.

2 Dynamic Model

We introduce a chemical reaction model with three dynamic variables [3], Li and Xu model, which includes two Michaelis-Menten reactions and exhibits chaotic behavior for certain parameter values. This model, described in Table 1.

Table 1: Kinetic expressions for reactions involving species X_1, X_2, and X_3, with rates expressed as functions of concentrations x_1, x_2, and x_3, and parameters k_i and K_{mi}

Reaction	Rate
$C_1 + X_1 \to 2X_1$	$k_1 x_1$
$2X_1 \to P$	$k_2 x_1^2$
$X_1 \to P$	$k_3 x_1 x_2/(x_1 + K_{m1})$
$X_2 \to P$	$k_4 x_2$
$C_2 + X_1 + X_2 \to X_1 + 2X_2$	$k_5 x_1 x_2$
$X_2 \to P$	$k_6 x_2 x_3/(x_2 + K_{m2})$
$X_3 \to P$	$k_7 x_3$
$C_3 + X_2 + X_3 \to X_2 + 2X_3$	$k_8 x_2 x_3$
$C_4 + X_3 \to 2X_3$	$k_9 x_3$

In this formulation, the system includes kinetic parameters denoted by k_j for $j = 1, \ldots, 9$, along with two Michaelis-type constants, indicated as K_{M_j} for $j = 1, 2$. The chemical entities labeled C_j (where $j = 1, \ldots, 4$) refer to reactants with fixed concentrations, and P designates the final product of the process. The dynamic variables x_j describe the time-dependent concentrations of intermediate species such as X_1, while the static concentrations of the A_j species are embedded within the values of the corresponding rate parameters. The set of reactions, as organized in Table 1, is assumed to proceed in a perfectly mixed, isothermal reactor environment.

Two enzyme-mediated mechanisms exhibiting Michaelis–Menten-type kinetics are distinguished: one governs the consumption of X_1 catalyzed by X_2, and the other governs the depletion of X_2 facilitated by X_3. Based on standard kinetic theory, the temporal evolution of the concentrations associated with X_1, X_2, and X_3 is governed by a coupled system of ordinary differential equations, derived from the reaction mechanisms described:

$$\begin{aligned}
\dot{x}_1 &= k_1 x_1 - k_2 x_1^2 - k_3 \frac{x_1 x_2}{x_1 + K_{m1}} \\
\dot{x}_2 &= -k_4 x_2 + k_5 x_1 x_2 - k_6 \frac{x_2 x_3}{x_2 + K_{m2}} \\
\dot{x}_3 &= -k_7 x_3 + k_8 x_2 x_3 + k_9 x_3
\end{aligned} \tag{1}$$

where $x = [x_1, x_2, x_3]$ corresponds to the concentration vector of the species involved, and $\dot{x} = [\dot{x}_1, \dot{x}_2, \dot{x}_3]$ describes the rate of change over time of these concentrations.

The kinetic parameters, including the Michaelis-Menten constants, are given as follows:

$$\begin{aligned}
&k_1 = 1, && k_2 = 1, && k_3 = 1, && k_4 = 0.25, \\
&k_5 = 0.625, && k_6 = 1, && k_7 = 0.25, && k_8 = 2.5,
\end{aligned} \tag{2}$$

$$k_9 = 0.028, \qquad K_{m1} = 0.2, \qquad K_{m2} = 0.05$$

The corresponding initial conditions are:

$$x_{10} = 0.1, \qquad x_{20} = 0.001, \qquad x_{30} = 0.1 \tag{3}$$

Fig. 1a–c illustrates that when the rate constants are selected according to Eqs. (2) and (3), the system exhibits chaotic behavior with persistent oscillations.

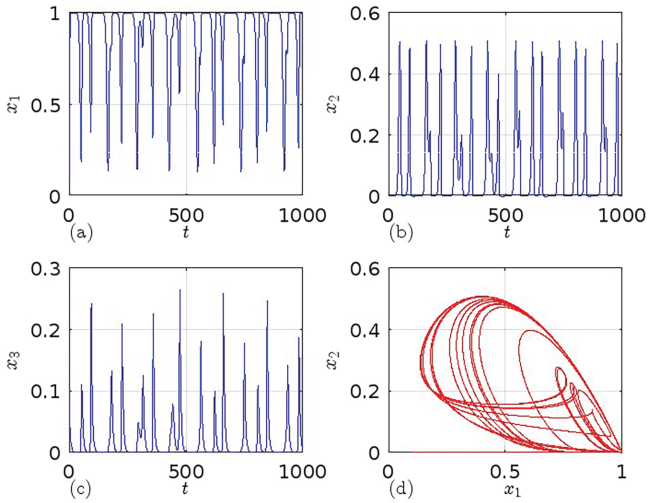

Figure 1: Dynamics of the chemical species over time: (a) evolution of X_1 concentration; (b) evolution of X_2 concentration; (c) evolution of X_3 concentration; (d) phase diagram showing the relation between x_1 and x_2

2.1 Determination of the Steady States

To determine the steady states of the system, each equation in (1) is set to zero, which corresponds to the condition where the concentrations of the chemical species no longer change with time.

$$\begin{aligned} &x_1 - x_1^2 - \frac{x_1 x_2}{x_1 + \frac{1}{5}} = 0 \\ &-\frac{1}{4}x_2 + \frac{5}{8}x_1 x_2 - \frac{x_2 x_3}{x_2 + \frac{1}{20}} = 0 \\ &-\frac{1}{4}x_3 + \frac{5}{2}x_2 x_3 + \frac{7}{250}x_3 = 0 \end{aligned} \tag{4}$$

- $(0, 0, 0)$ is the trivial steady state.
- If $x_2 = x_3 = 0$, then $x_1 = 1$, so $(1, 0, 0)$ is a steady state.
- If $x_3 = 0$, then from the second equation: $-x_2\left(\frac{1}{4} - \frac{5}{8}x_1\right) = 0$, which implies $x_1 = \frac{2}{5}$. Substituting into the first equation yields the steady state $\left(\frac{2}{5}, \frac{9}{25}, 0\right)$.

Additional steady states can be computed numerically using MATLAB's *fsolve* routine; for example, one such approximate solution is $x^* = (0.9208,\ 0.0888,\ 0.0452)$.

The Jacobian matrix of the system described by Eq. (1), evaluated at the steady-state point x^*, yields the following set of eigenvalues:

$$\lambda_1 = -0.7953 \qquad \lambda_{2,3} = 0.1009 \pm 0.2958i \tag{5}$$

Therefore, x^* is classified as a saddle-focus point and is unstable [15]. Moreover, since all eigenvalues have nonzero real parts, x^* is a hyperbolic point, which ensures that the linearization accurately captures the local dynamics. This configuration may be associated with the emergence of chaotic behavior, which can be further confirmed by computing the Lyapunov exponents.

2.2 Lyapunov Exponents and Fast Fourier Transform (FFT)

The dynamics of the system described by Eq. (1) can be characterized through its Lyapunov exponents, computed using Eqs. (2) and (3). We apply Wolf's method [12] to calculate the Lyapunov exponents. The Lyapunov spectrum of the system is $[+, 0, -]$:

$$\Lambda_1 = 0.016; \qquad \Lambda_2 \approx 0; \qquad \Lambda_3 = -0.742 \tag{6}$$

The presence of a positive Lyapunov exponent in the spectrum (6) confirms that the three-variable chemical reaction model exhibits chaotic dynamics. This positive exponent also suggests the existence of a strange attractor, which is consistent with the phase diagram shown in Fig. 1d.

The sum of the exponents is ($\sum_{i=1}^{3} \Lambda_i = -0.726 < 0$), indicating that the system is dissipative and confirming phase space contraction [16].

The frequency spectra (see Fig. 2) exhibit a prominent peak at zero frequency, indicating the presence of a strong direct current (DC). Additionally, the surrounding energy distribution, marked by multiple peaks with no regular spacing, points to a chaotic dynamic. This behavior contrasts with that of purely periodic systems, which typically display sharply defined and regularly spaced spectral peaks.

2.3 Poincaré Maps

When $k_9 = 0.028$, the system presents clear signs of chaotic dynamics, as evidenced by the irregular scattering observed in the Poincaré maps. The dynamic analysis depicted in Fig. 3 reinforces this conclusion, revealing complex and unpredictable trajectories in the phase space. These paths lack periodic behavior or convergence to stable cycles, instead displaying a highly intricate and erratic structure. The scattered distribution of points, devoid of symmetry or recognizable patterns, is a hallmark of chaos typically associated with strange attractors–geometrical structures that reflect the system's sensitivity to initial conditions [17]. Similar approaches using Poincaré maps have been applied to investigate nonlinear dynamics and steady-state stability in fractional-order systems [18].

On the other hand, for $k_9 = 0.25$, the system converges to either a fixed point or a stable periodic orbit, exhibiting organized and structured Poincaré maps. In systems with periodic or quasi-periodic behavior, Poincaré maps typically display well-defined patterns, such as discrete clusters or smooth closed curves. The Lyapunov exponents for $k_9 = 0.25$, given as $[-0.227, -0.994, -1.627]$, indicate that the system is governed by a fixed-point attractor. This interpretation is further supported by the frequency spectrum of the state variable x_3 (see Fig. 4), which reveals a prominent and narrow peak centered near zero frequency. Such a spectral profile suggests minimal oscillatory activity or

convergence to a steady-state value, reinforcing the conclusion that the system evolves toward a non-chaotic and stable dynamical regime.

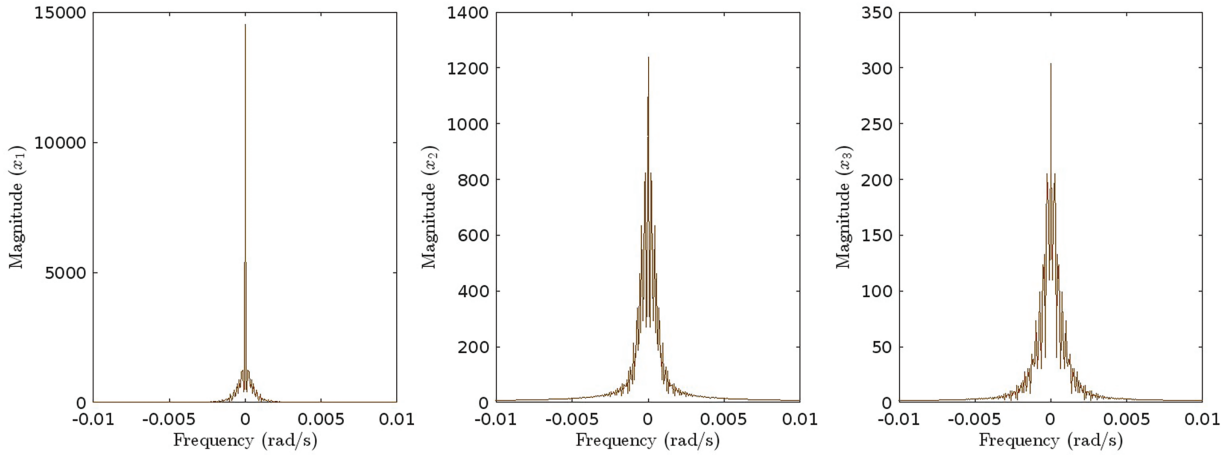

Figure 2: Frequency spectra of the state variables x_1, x_2, and x_3, obtained via FFT

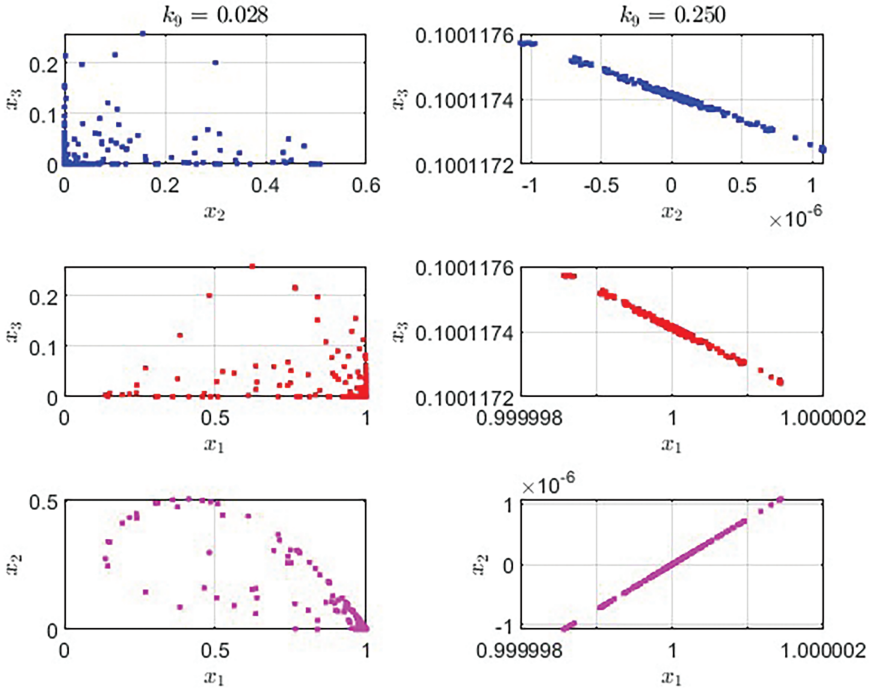

Figure 3: Poincaré maps for the planes: $x_1 = 0$ (blue), $x_2 = 0$ (red), and $x_3 = 0$ (magenta) for different values of the parameter k_9

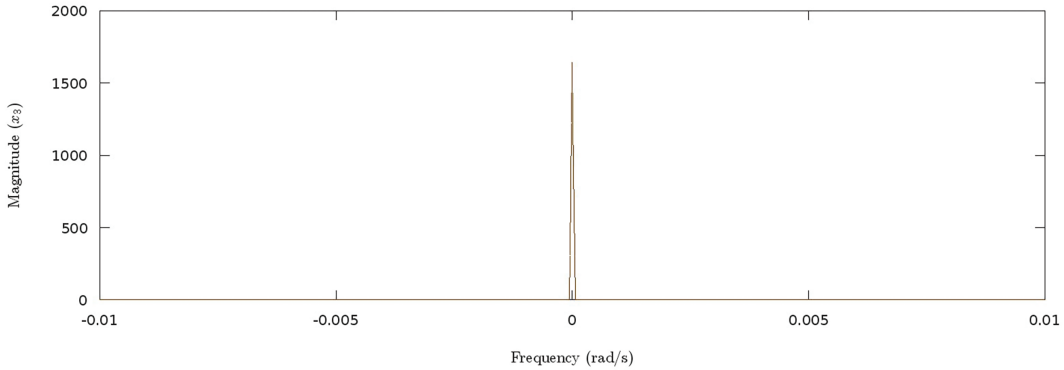

Figure 4: Frequency spectra of the state variable x_3 and $k_9 = 0.25$, obtained via FFT

3 Parameter Uncertainty Characterization

When analyzing nonlinear chemical reaction systems, it's important to consider that model parameters may not be known precisely. Variations often arise due to measurement inaccuracies or the inherent complexity of chemical kinetics. A common way to deal with this issue is by introducing uncertainty into the parameters, typically through bounded intervals or probabilistic descriptions [19–21].

Since computer simulations are deterministic by nature, we can't rely on genuine randomness. Instead, we use pseudo-random number generators to simulate variability. In this study, we adopt the approach described by L'Ecuyer [22], which generates pseudo-random sequences using recurrence relations defined over a finite state space.

To introduce variability into the kinetic parameters of our system, we used the `rand` function available in MATLAB® R2024a, which randomly draws samples from a uniform distribution on the interval ([0, 1]). Each parameter (k) was perturbed according to the following expression:

$$\bar{k} = k(0.8 + 0.4p(t)) \tag{7}$$

Here, in Eq. (7), $p(t) \sim \mathcal{U}[0, 1]$ represents a pseudo-random value at a given time step, allowing the parameter to fluctuate by up to ±20% relative to its nominal value.

Table 2 lists the parameters from the current three-variable model that were considered uncertain in the simulations.

Table 2: Uncertain parameters in the 3-D system

Nominal parameters	Perturbed parameters
$k_1 = 1$	$\bar{k}_1 = 0.8 + 0.4p(t)$
$k_2 = 1$	$\bar{k}_2 = 0.8 + 0.4p(t)$
$k_3 = 1$	$\bar{k}_3 = 0.8 + 0.4p(t)$
$k_4 = 0.25$	$\bar{k}_4 = 0.2 + 0.1p(t)$
$k_5 = 0.625$	$\bar{k}_5 = 0.5 + 0.25p(t)$

(Continued)

Table 2 (continued)

Nominal parameters	Perturbed parameters
$k_6 = 1$	$\bar{k}_6 = 0.8 + 0.4p(t)$
$k_7 = 0.25$	$\bar{k}_7 = 0.2 + 0.1p(t)$
$k_8 = 2.5$	$\bar{k}_8 = 2 + p(t)$
$k_9 = 0.028$	$\bar{k}_9 = 0.0224 + 0.0112p(t)$
$K_{m1} = 0.2$	$\bar{K}_{m1} = 0.16 + 0.08p(t)$
$K_{m2} = 0.05$	$\bar{K}_{m2} = 0.04 + 0.02p(t)$

4 Optimal Linear Control Strategy

This study employs the optimal linear control framework originally developed by Rafikov and Balthazar [11] to stabilize the nonlinear chemical reaction system under investigation. The primary objective of this method is to design a state-feedback control law capable of guiding the system from an arbitrary initial condition toward a predefined reference trajectory, while simultaneously minimizing a quadratic cost functional.

The dynamics of the controlled system are expressed as:

$$\dot{x} = Ax + g(x) + Bu, \tag{8}$$

where $x \in \mathbb{R}^n$ denotes the state vector, $A \in \mathbb{R}^{n\times n}$ is a constant matrix representing the linear part of the system, $g(x)$ accounts for the nonlinearities, $B \in \mathbb{R}^{n\times m}$ is the control input matrix, and $u \in \mathbb{R}^m$ is the control vector.

The control strategy is constructed around a reference trajectory $\tilde{x} \in \mathbb{R}^n$, which in this application is chosen as the origin, i.e., $\tilde{x} = [0 \;\; 0 \;\; 0]^T$. Introducing the deviation variable $y = x - \tilde{x}$, the system is recast in terms of the tracking error:

$$\dot{y} = Ay + G(y)y + Bu, \tag{9}$$

where $G(y)$ captures the contribution of the nonlinear dynamics, typically approximated around the steady state.

To synthesize the control input, a quadratic performance index is considered:

$$\tilde{J} = \int_0^\infty \left(y^\top \tilde{Q} y + u^\top R u \right) dt, \tag{10}$$

where $\tilde{Q} = Q - G^\top(y)P - PG(y)$, with $Q \in \mathbb{R}^{n\times n}$ and $R \in \mathbb{R}^{m\times m}$ being symmetric positive-definite weighting matrices. These matrices reflect the trade-off between state regulation and control effort.

Minimization of the cost functional leads to the feedback control law:

$$u(t) = -Ky(t), \tag{11}$$

where $K = R^{-1}B^\top P$, and P is the unique symmetric positive-definite solution of the algebraic Riccati equation:

$$PA + A^\top P - PBR^{-1}B^\top P + Q = 0. \tag{12}$$

The resulting control law stabilizes the origin locally in the presence of nonlinearities. Under mild assumptions on the boundedness of $G(y)$ and with an appropriate choice of the weighting matrices, global asymptotic stability can also be achieved. This approach ensures that the closed-loop system exhibits robust performance, even in the presence of nonlinear behavior.

The full procedure adopted in this study is summarized in the diagram shown in Fig. 5. It outlines the implementation steps of the optimal linear control strategy, from solving the algebraic Riccati equation to verifying the positive definiteness of the matrix $\tilde{Q}$, that is, $\tilde{Q} \succ 0$. This iterative process ensures the stabilization of the nonlinear dynamics while minimizing the cost functional defined in Eq. (10).

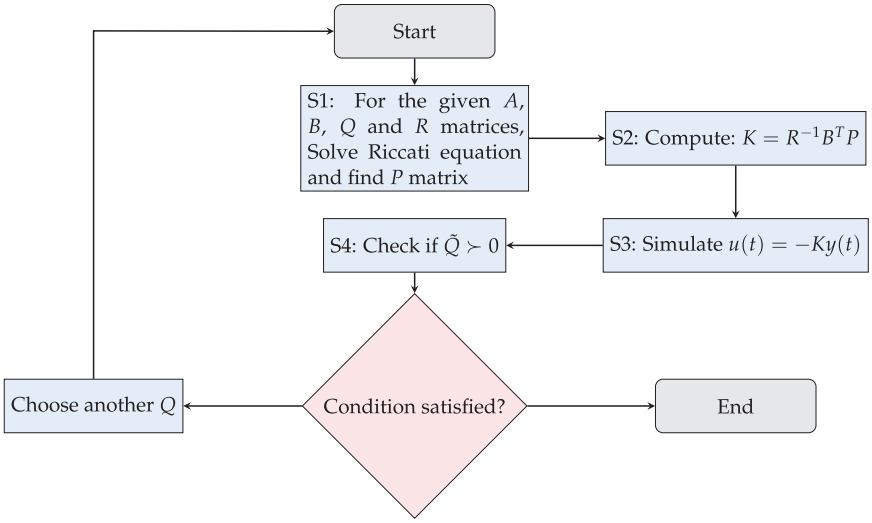

Figure 5: Diagram of the optimal linear controller synthesis

5 Results Numerical and Discussion

Numerical experiments were conducted to evaluate the performance of the proposed control strategy. The simulations were performed using the ODE45 solver available in MATLAB® R2024a, applied to the dynamic model of the chemical reaction system (1), considering the parametric and initial conditions previously defined in Eqs. (2) and (3), respectively.

5.1 State-Feedback Control of the Chemical System with Nominal Parameters

The following matrices define the linearized dynamics and control structure of the system:

$$A = J(x^*) = \begin{bmatrix} -0.8426 & -0.9893 & 0 \\ 0.0555 & 0.2491 & -0.8162 \\ 0 & 0.1130 & 0 \end{bmatrix} \tag{13}$$

The input matrix B, output error y, reference state $\tilde{x}$, and weighting matrices Q and R used in the optimal linear control design are given as:

$$B = \begin{bmatrix} 1 \\ 1 \\ 0 \end{bmatrix}, \quad y = \begin{bmatrix} x_1 - \tilde{x}_1 \\ x_2 - \tilde{x}_2 \\ x_3 - \tilde{x}_3 \end{bmatrix}, \quad \tilde{x} = \begin{bmatrix} 0 \\ 0 \\ 0 \end{bmatrix}, \quad Q = \begin{bmatrix} 1 & 0 & 0 \\ 0 & 1 & 0 \\ 0 & 0 & 1 \end{bmatrix}, \quad R = [1] \tag{14}$$

To ensure controllability, we verify that the controllability matrix $\mathcal{C} = [B\ AB\ A^2B]$ has full rank, i.e., rank 3 for a third-order system. With this confirmed, the continuous-time algebraic Riccati equation is solved numerically using MATLAB® R2024a, resulting in the following symmetric positive-definite matrix:

$$P = \begin{bmatrix} 0.5561 & -0.5653 & 0.5711 \\ -0.5653 & 2.4000 & 0.2247 \\ 0.5711 & 0.2247 & 34.7544 \end{bmatrix} \tag{15}$$

The resulting optimal feedback gain matrix K, used to define the control law $u(t) = -Kx(t)$, is:

$$K = \begin{bmatrix} -0.0092 & 1.8344 & 0.7958 \end{bmatrix} \tag{16}$$

Thus, the control input that minimizes the quadratic cost is explicitly given by:

$$u(t) = -0.0092x_1 + 1.8344x_2 + 0.7958x_3 \tag{17}$$

Fig. 6 illustrates the dynamic response of the system under the application of the proposed control strategy. The time series of the state variables x_1, x_2, and x_3 (Fig. 6a–c) show that, after a brief transient period, the variables converge to constant values, indicating the stabilization of the system at a steady state. The projections onto two-dimensional planes (Fig. 6d–f) further confirm this behavior, as the trajectories smoothly converge to a single fixed point in the phase space. These results highlight the effectiveness of the control strategy in suppressing chaotic oscillations and stabilizing the dynamics of the chemical system.

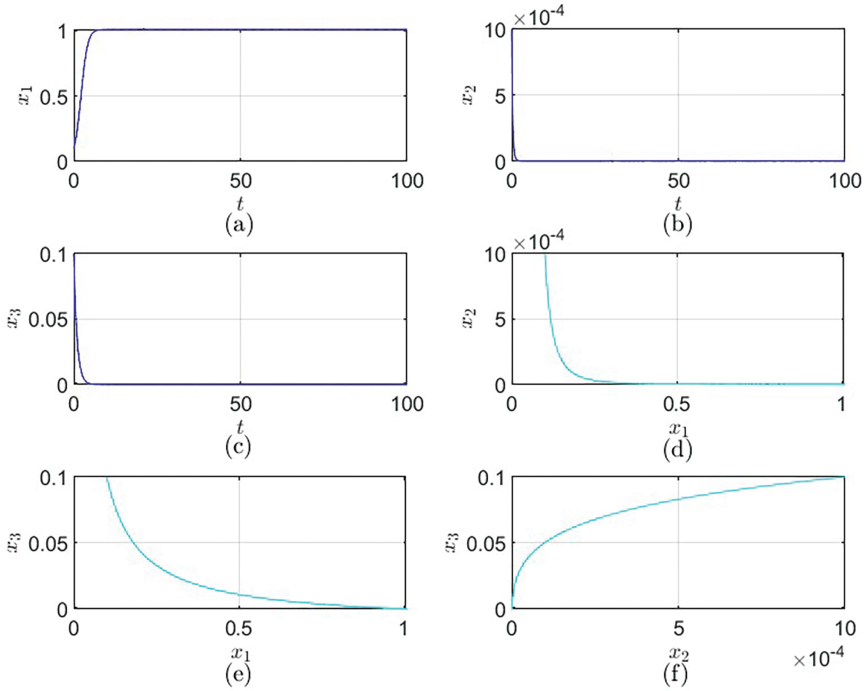

Figure 6: Dynamics of the chemical species under control action: (a) evolution of X_1 concentration; (b) evolution of X_2 concentration; (c) evolution of X_3 concentration; (d) phase diagram showing the relation between x_1 and x_2; (e) phase diagram of x_1 vs. x_3; (f) phase diagram of x_2 vs. x_3

The control signal (Eq. (17)) is applied to the system to correct the deviation from the desired state. Initially, the control signal takes a negative value, indicating an initial correction to compensate for the state deviation. Over time, the signal decreases in magnitude and, by around $t = 40\,\text{s}$, it approaches a constant positive value of approximately 0.04. This behavior indicates that the system has been effectively guided to a steady state without significant oscillations. Fig. 7 illustrates this evolution of the control signal.

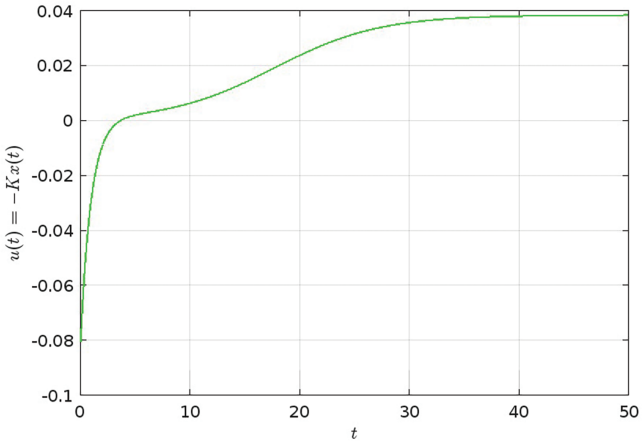

Figure 7: Control signal $u(t)$

The results presented in Table 3, along with Fig. 8, demonstrate that the average convergence time increases as the tolerance ϵ becomes more stringent. This behavior is primarily driven by the stabilization time of the variable x_1, which remains high across all tolerance levels. In contrast, x_2 stabilizes almost instantaneously, while x_3 shows a moderate sensitivity to the tolerance parameter, exhibiting a gradual increase in convergence time. Additionally, the rise in average convergence time does not follow a linear pattern, suggesting an increasing sensitivity of the system as the convergence criterion becomes stricter.

Table 3: Convergence times (in seconds) for each tolerance and the mean

Tolerance ϵ	x_1 (s)	x_2 (s)	x_3 (s)	Mean (s)
0.10	28.50	0.01	0.01	9.5067
0.05	29.20	0.01	0.69	9.9667
0.01	29.84	0.01	2.27	10.7070

5.2 State-Feedback Control of the Chemical System with Perturbed Parameters

In this section, we adopt the matrices defined in (14), except for matrix A, which is now given by:

$$A = \begin{bmatrix} -1.2311 & -0.8013 & 0 \\ 0.0661 & 0.2919 & -0.6333 \\ 0 & 0.0937 & -0.0407 \end{bmatrix} \tag{18}$$

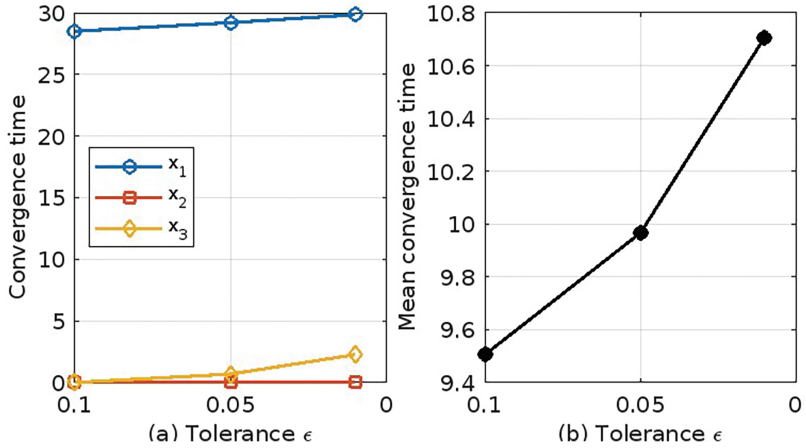

Figure 8: Convergence time of the control. (a) Convergence time vs. tolerance. (b) Mean convergence time vs. tolerance

Based on these parameters, the solution of the algebraic Riccati equation yields the matrix P and the optimal feedback gain matrix K, given by:

$$P = \begin{bmatrix} 0.3871 & -0.3109 & 0.1472 \\ -0.3109 & 1.9208 & -0.1495 \\ 0.1472 & -0.1495 & 14.6083 \end{bmatrix} \quad \text{and} \quad K = \begin{bmatrix} 0.0762 & 1.6098 & -0.0023 \end{bmatrix} \tag{19}$$

The dynamic response of the system under the proposed control strategy is contrasted in Fig. 9, where the behavior with uncertain parameters (solid curves) is compared to that with fixed parameters (dashed curves). Notably, when parameters are uncertain, the transient responses differ slightly—convergence may occur somewhat slower or faster—demonstrating the impact of parameter variability on system dynamics.

Nonetheless, the two-dimensional projections (Fig. 9d–f) show that, regardless of parameter certainty, the trajectories ultimately coalesce at a single fixed point in phase space. This observation underscores the robustness of the control strategy: even when key parameters deviate from their nominal values, the controller effectively suppresses chaotic oscillations and stabilizes the system. Overall, these results confirm that the proposed approach successfully eliminates chaotic behavior under ideal conditions and maintains stabilization in the presence of parameter uncertainty.

6 Conclusion

In this study, an optimal linear control strategy was applied to stabilize a nonlinear chemical reaction system exhibiting chaotic behavior. The system's dynamics, characterized by strong nonlinearities and sensitivity to initial conditions, pose additional challenges to stabilization, especially in the presence of parametric uncertainties.

The control strategy, based on the methodology proposed by Rafikov and Balthazar, employs a state-dependent feedback law derived from solving an algebraic Riccati equation, minimizing a quadratic performance index. Numerical simulations and dynamical analysis tools—such as Lyapunov exponents, FFT, and Poincaré maps—validated the effectiveness of the proposed control approach.

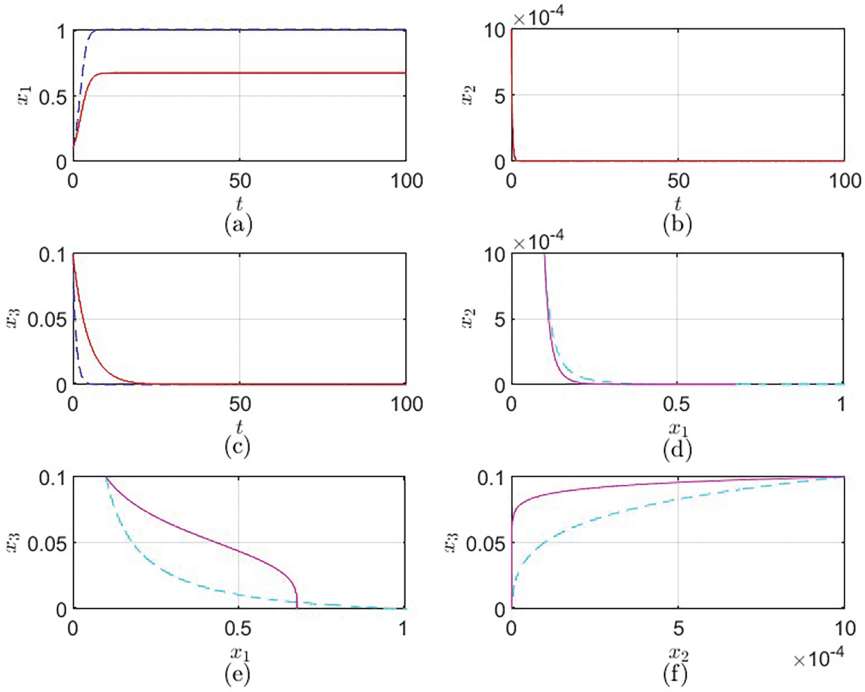

Figure 9: Dynamics of the chemical species under parameter uncertainty and control action: (a) evolution of X_1 concentration; (b) evolution of X_2 concentration; (c) evolution of X_3 concentration; (d) phase diagram showing the relation between x_1 and x_2; (e) phase diagram of x_1 vs. x_3; (f) phase diagram of x_2 vs. x_3

The key conclusions of this study are as follows:

- Effective stabilization of chaotic chemical systems: The results demonstrated that the proposed controller successfully suppressed chaotic oscillations, driving the system toward equilibrium both under fixed parameters and parametric uncertainties of up to 20%. As shown in Figs. 6 and 9, the state variables (x_1, x_2, x_3) converge to constant values, confirming stabilization.
- Robustness of the optimal linear control strategy: The control approach proved to be resilient to parameter variations, reinforcing its applicability in real-world scenarios where precise parameter knowledge cannot always be guaranteed. Fig. 9 illustrates that the system stabilizes even when parameters deviate significantly, ensuring reliable performance under uncertainty.
- Practical applicability and computational feasibility: The control signal, shown in Table 3 and Fig. 8b, indicates that the average convergence time remains between 9.5 and 10.7 s depending on the tolerance criteria, demonstrating efficiency in achieving equilibrium.
- Energetic efficiency of the control action: As depicted in Fig. 7, the control signal settles into a small, steady value of approximately 0.04 after t = 40 s, indicating that the system is maintained in equilibrium with minimal effort. This underscores the method's practical value, especially in systems where energy efficiency is a priority.
- Contribution to nonlinear system control: This study bridges the gap between classical optimal control and chaotic chemical systems, demonstrating that robust stabilization can be achieved even in highly nonlinear dynamic environments. Furthermore, the stabilization time for x_1

remains close to 29 s across different tolerances, while x_2 and x_3 converges nearly instantly (Fig. 8a and Table 3).

By confirming the efficacy and robustness of optimal linear control in this context, this research provides valuable insights into controlling chaotic chemical processes, opening opportunities for further investigation into applications in engineering and process optimization.

Acknowledgement: The authors express their sincere gratitude to UEMS and UNESP for their valuable support.

Funding Statement: This study did not receive external funding.

Author Contributions: The authors confirm contribution to the paper as follows: Conceptualization, Marcio Demetrius Martinez and Fábio Roberto Chavarette; Methodology, Marcio Demetrius Martinez and Fábio Roberto Chavarette; Software, Marcio Demetrius Martinez; Validation, Marcio Demetrius Martinez and Fábio Roberto Chavarette; Formal analysis, Marcio Demetrius Martinez; Investigation, Marcio Demetrius Martinez; Resources, Marcio Demetrius Martinez; Data curation, Marcio Demetrius Martinez; Writing—original draft preparation, Marcio Demetrius Martinez; Writing—review and editing, Fábio Roberto Chavarette; Visualization, Marcio Demetrius Martinez; Supervision, Fábio Roberto Chavarette; Project administration, Fábio Roberto Chavarette. All authors reviewed the results and approved the final version of the manuscript.

Availability of Data and Materials: The data supporting the findings of this study are available from the corresponding author upon reasonable request.

Ethics Approval: This study did not involve any experiments with human participants or animals.

Conflicts of Interest: The authors declare no conflicts of interest to report regarding the present study.

References

1. Anwar MS, Alqarni MS, Irfan M. Exploring the marvels of heat transfer: MHD convection at a stagnation point in non-Newtonian fluid with yield stress and chemical reactions. Chin J Phys. 2024;89:1299–308. doi:10.1016/j.cjph.2024.01.030.
2. Bodale I, Oancea VA. Chaos control for Willamowski-Rössler model of chemical reactions. Chaos Soliton Fract. 2015;78(31):1–9. doi:10.1016/j.chaos.2015.06.019.
3. Li QS, Xu W. Chaos in a three-variable chemical reaction model. J Chem Res. 2001;2001(11):474–5. doi:10.3184/030823401103168532.
4. Martinez MD, Chavarette FR. Managing chaos in chemical reactions with uncertain system parameters: exploring 4-D hyperchaotic system. SeMA J. 2025;82(1):1–16. doi:10.1007/s40324-025-00385-9.
5. Killory H, Rössler OE, Hudson JL. Higher chaos in a four-variable chemical reaction model. Phys Lett A. 1987;122(6–7):341–5. doi:10.1016/0375-9601(87)90839-5.
6. Katsanikas M, Agaoglou M, Montoya FG. Introduction to special issue: chaos indicators, phase space and chemical reaction dynamics. Physica D. 2022;439:445.
7. Rashid M, Irfan M, Muhammad T, Abu-Jrai A, Anwar MS. Dynamics of solar radiation absorption for Darcy-Forchheimer Carreau nanofluid considering variable conductivity with chemical reaction: a solar thermal energy application. Results Eng. 2025;26:104670. doi:10.1016/j.rineng.2025.104670.

8. Nolasco E, Vassiliadis VS, Kähm W, Adloor SD, Al Ismaili R, Conejeros R, et al. Optimal control in chemical engineering: past, present and future. Comput Chem Eng. 2021;155(9):107528. doi:10.1016/j.compchemeng.2021.107528.
9. Aguilar-López R. Chaos suppression via Euler-Lagrange control design for a class of chemical reacting system. Math Probl Eng. 2018;2018(2):3802801. doi:10.1155/2018/3802801.
10. Mahdy AMS, Higazy M. Numerical different methods for solving the nonlinear biochemical reaction model. Int J Appl Comput Math. 2019;5(6):148. doi:10.1007/s40819-019-0740-x.
11. Rafikov M, Balthazar JM. On control and synchronization in chaotic and hyperchaotic system via linear control feedback. Nonlinear Sci Numer Simul. 2008;13(7):1246–55. doi:10.1016/j.cnsns.2006.12.011.
12. Wolf A, Swift JB, Swinney HL, Vastano JA. Determining Lyapunov exponents from a time series. Physica D. 1985;16(3):285–317. doi:10.1016/0167-2789(85)90011-9.
13. Alligood K, Sauer T, Yorke J. Chaos: an introduction to dynamical systems. New York, NY, USA: Springer; 1996. doi:10.1007/b97589.
14. Zandi-Mehran N, Nazarimehr F, Rajagopal K, Ghosh D, Jafari S, Chen G. FFT bifurcation: a tool for spectrum analyzing of dynamical systems. Appl Math Comput. 2022;422:126986. doi:10.1016/j.amc.2022.126986.
15. Vaidyanathan S, He S, Sambas A. A new multistable double-scroll 4-D hyperchaotic system with no equilibrium point, its bifurcation analysis, synchronization and circuit design. Arch Control Sci. 2021;31(1):99–128. doi:10.24425/acs.2021.136882.
16. Nikravesh SKY. Nonlinear systems stability analysis: Lyapunov-based approach. 1st ed. Boca Raton, FL, USA: CRC Press; 2018. 319 p. doi:10.1201/9781315215990.
17. Norouzi H, Younesian D. Fluid-structure interactions in nonlinear plates subjected to sub and supersonic airflow: a review. Thin-Walled Struct. 2023;192(8):111144. doi:10.1016/j.tws.2023.111144.
18. Mahdy AMS. Stability, existence, and uniqueness for solving fractional glioblastoma multiforme using a Caputo-Fabrizio derivative. Math Methods Appl Sci. 2025;48(7):7360–77. doi:10.1002/mma.9038.
19. Moffat RJ. Describing the uncertainties in experimental results. Exp Therm Fluid Sci. 1988;1(1):3–17. doi:10.1016/0894-1777(88)90043-X.
20. Didier J, Faverjon B, Sinou JJ. Analysing the dynamic response of a rotor system under uncertain parameters by polynomial chaos expansion. J Vib Control. 2012;18(5):712–32. doi:10.1177/1077546311404269.
21. Chavarette FR. Optimal linear control to parametric uncertainties in a micro electro mechanical system. Int J Pure Appl Math. 2013;83(4):539–48.
22. L'Ecuyer P. Uniform random number generation. Ann Oper Res. 1994;53(1):77–120. doi:10.1007/BF02136827.